ROBUST ELECTRICAL TRANSFER SYSTEM (RETS) FOR SOLAR ARRAY DRIVE MECHANISM SLIPRING ASSEMBLY

Daniel Bommottet [(1)], Luc Bossoney[(2)], Ralph Schnyder [(3)], Alan Howling[(3)], Christoph Hollenstein[(3)]

[(1)] RUAG Space, ch. De la Vuarpillière 29 – 1260 Nyon - Switzerland,
Email:daniel.bommottet@ruag.com
[(2)] HEIG-VD-IESE, 1400 Yverdon-Les-Bains, Switzerland,
Email:luc.bossoney@heig-vd.ch
[(3)] EPFL-Centre de Recherche en Physique des Plasmas, 1015 Lausanne, Switzerland,
Emails: ralph.schnyder@epfl.ch, christoph.hollenstein@epfl.ch, alan.howling@epfl.ch

ABSTRACT

Demands for robust and reliable power transmission systems for sliprings for SADM (Solar Array Drive Mechanism) are increasing steadily. As a consequence, it is required to know their performances regarding the voltage breakdown limit.
An understanding of the overall shape of the breakdown voltage versus pressure curve is established, based on experimental measurements of DC (Direct Current) gas breakdown in complex geometries compared with a numerical simulation model.

In addition a detailed study was made of the functional behaviour of an entire wing of satellite in a like-operational mode, comprising the solar cells, the power transmission lines, the SRA (SlipRing Assembly), the power S3R (Sequential Serial/shunt Switching Regulators) and the satellite load to simulate the electrical power consumption.

A test bench able to measure automatically the: a)breakdown voltage versus pressure curve and b)the functional switching performances, was developed and validated.

1. INTRODUCTION

The RETS project was split in three distinct phases:

1. Laboratory experimental study.
2. Electrical modelling of satellite PSS (Power Supply System). Simulations of relevant situations.
3. Development and validation of a test bench. Qualification of a slipring for SADM.

The goal of the activity is at the end to have a test bench to perform high voltage measurements, functional switching tests, and to propose design guidelines to the Primes satellites manufacturers.

The SRA for SADM are used for power transmission from solar panels to the satellite PCU (Power Control Unit). It is composed of many conducting rings separated by insulators and associated slipping brushes allowing the current transfer during the rotation. The voltage difference between conducting rings respectively brushes may lead to arcing and possible failures. The power transmission in a satellite PSS requires knowing the breakdown limits.
An understanding of breakdown may lead to new designs, and highlight the working limits of the components, or suggest design modifications to improve future devices. In fact, the PSS should being developed and configured to withstand higher voltages at smaller dimensions without gas breakdown over a large pressure range (from atmospheric pressure on earth to high vacuum in space).

DC breakdown in complicated assemblies is hard to predict especially over a large pressure range. Most breakdown investigations assumed simple geometries like parallel plates and pin to plate.

In the present work we investigate DC breakdown in various gases for a slipring assembly. Breakdown voltage versus pressure for a ring assembly shows a similar shaped curve to the well-known Paschen curve for a parallel plate geometry. Moreover, optical spectroscopy provides additional information to distinguish between the different breakdown mechanisms depending on gas pressure. To understand the breakdown voltage versus pressure dependence a numerical model was developed for gas breakdown. Double gap geometry is then used to show the importance of the longest and shortest electric field path lengths in determining the low and high pressure thresholds. Next, a multi-gap geometry adds the understanding of the extended pressure range of minimum breakdown voltage compared to the simple Paschen curve.
Finally, the numerical simulation of a ring assembly geometry compared to experimental measurements highlights the main parameters, which influence the calculated breakdown voltages, and gives a new view on breakdown in a complex geometry.
Besides the laboratory experimental study, a macroscopic approach is proposed, where the complete wing of a satellite is modelled and simulated. The

numerical results are confirmed by experimental measurements on representative hardware. These simulation and tests have permit to understand the interaction between the different electrical components of a PSS that are mainly the solar cells, the cabling, the slipring assembly and the S3R. The lessons learned will lead to improve the reliability of the future designs.

A complete automated test bench was developed and will permit to test the SRA in representative situations of environment and functioning.

A full qualification of a SRA for SADM was performed successfully with the developed test bench.

2. EXPERIMENTAL STUDY

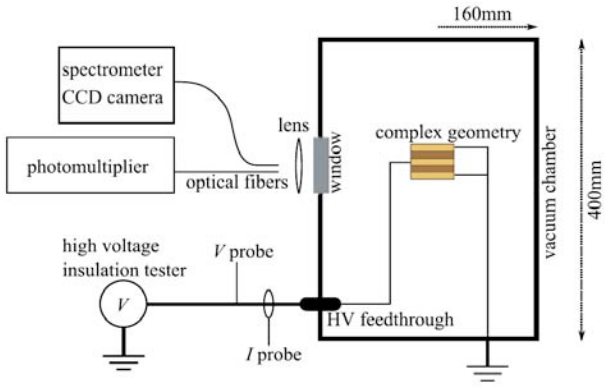

Figure 1. Schematic drawing of the experimental setup. The assembly of five rings is placed in the middle of the cylindrical vacuum chamber. The electrodes are brass rings: the top and bottom rings are grounded and the middle ring is at high voltage. The insulator rings are of Ultem® resin.

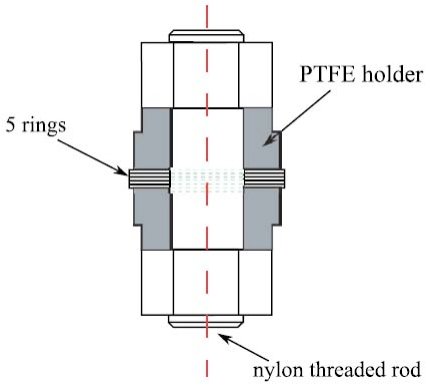

Figure 2. Schematic of the ring assembly and PTFE holder.

2.1. DESCRIPTION

The SRA was substituted by a representative ring geometry composed of only five rings as shown in Figure 1 and Figure 2. The top and bottom rings are grounded whereas the middle one is at high voltage. The rings in between are insulation rings. An epoxy structural adhesive (ScotchWeld 2216 B/A) is used to cover the soldered connection between the metal rings and the wires. The ring assembly is held together by a PTFE holder and the internal volume is filled by the nylon threaded rod. It is placed in the middle of the grounded cylindrical vacuum chamber.

Measurements were performed over wide pressure ranges (from 2×10^{-5} to 10^{3} mbar) with different gases.

It was chosen to start measurements with a pressure as low as possible in order to avoid air contamination, especially for experiments with gases such as argon.

A non-destructive high voltage insulation tester is used to apply voltages up to 30 kVdc. No external resistance was necessary to avoid high current damage because the tester current limit is set as low as 100 μA. The voltage and current are measured with fast instrumentation. An optical fiber and lens directed towards the electrodes and connected to a photomultiplier provides light intensity measurement. When breakdown occurs, electron and ion densities grow rapidly leading to a rapid increase of current and light intensity. The breakdown was triggered on the appearance of either current or light.

The threshold value was adjusted according to the kind of breakdown. Current and voltage oscillations were observed after breakdown, especially for high-pressure arcs and for vacuum discharges. In order to determine the breakdown voltage as a function of the pressure, the pressure is set first. Once the pressure is stable in the vacuum chamber, the voltage is increased starting from 0V until breakdown detection. To avoid any significant overvoltage, the voltage ramp was at a low rate of about 200 Vs^{-1}. To study the optical emission spectrum of the discharges following the breakdown an optical spectrometer with a 0.3 nm resolution and equipped with a CCD (Charge-Coupled Device) camera is used.

2.2. RESULTS and DISCUSSION

2.2.1. Breakdown voltage versus pressure curves

Over the large pressure range investigated two kind of discharges are found: gas and vacuum discharges. In the gas discharges the breakdown mechanism starts with a free electron which is accelerated by the electric field, ionizes the gas and leads to an avalanche. Then a secondary electron emission is needed to obtain dc breakdown. On the other hand, vacuum breakdown occurs at very low pressures where ionization collisions are rare. Nevertheless electron emission current in a strong electric field can produce a sufficient amount of medium (metal vapour or desorbed gas) for the breakdown to develop as a gas breakdown (avalanche and secondary emission). Vacuum discharges are highly dependent on electrode surface condition. Each breakdown discharge removes electrode protrusions, micro defects, attached gas molecules or contaminants or even damages the surface. This conditioning which modifies the surface of the electrode with each discharge impacts on further breakdown voltage measurements.

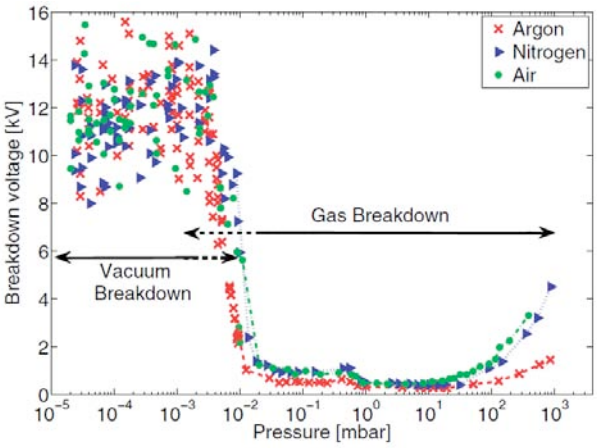

Figure 3. Measured dc breakdown voltages for the ring assembly from 2 × 10^{-5} to 10^{3} mbar in different gases.

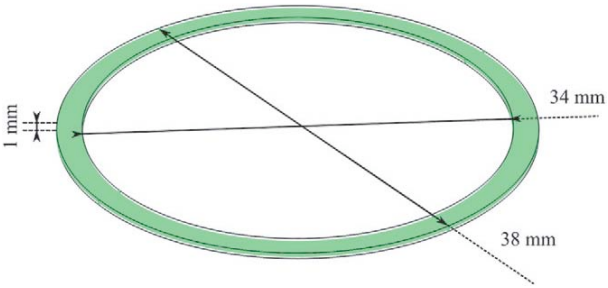

Figure 4. Scale drawing of the rings. The ring edges have a 0.1mm radius of curvature. The surface finish of the conductors is N7 (roughness value Ra = 1.6μm).

In Paschen curves for simple geometries such as parallel plates, breakdown voltages are expressed according to the product of gas pressure and gap width between electrodes.

Since the ring assembly does not have a well-defined gap, it is not possible to express the breakdown voltages according to pressure times gap as in Paschen curves. We measured dc breakdown voltages for the ring assembly geometry for gas pressures from 2 × 10^{-5} to 10^{3} mbar in different gases as a function only of gas pressure (see Figure 3).

Two distinct mechanisms are seen over the large gas pressure range: vacuum discharges occur at low pressures, whereas gas discharges dominate at high pressures. In the transition zone between 10^{-3} and 10^{-2} mbar both types of discharges can be present. The huge increase of breakdown voltage in this pressure zone defined the so-called critical pressure.

In the vacuum discharge range (10^{-5} to 10^{-3} mbar) the breakdown voltages are dispersed even for the same pressure and are independent of gas type showing a clear difference between the two kinds of discharges. The spread in breakdown voltages could be partly due to surface conditioning effects or overvoltage caused by a too rapid voltage ramp. Above 10^{-3} mbar, gas discharge processes need to be taken into account. From 10^{-2} to 10^{3} mbar the gas discharge breakdown voltage curve looks similar to a Paschen curve for each gas tested.

In contrast to vacuum discharges, the gas breakdown voltage at a given pressure is fairly reproducible because the ionization mechanism in the gas and the secondary processes are not strongly modifying the surface condition. Apart from the thresholds at high pressure and low pressure, a wide pressure range from about 0.1 to 10 mbar shows almost constant breakdown voltage values. The wide flat shape is due to the many possible electric field path lengths present in the ring assembly geometry.

The overall shape of the breakdown voltage versus pressure curve remains the same for all tested gases with the vacuum breakdown voltage always higher than for gases.

At high pressures, the discharge is observed to occur between the rings in the form of an arc. As the pressure is decreased the arc becomes more diffuse and gradually covers the grounded rings. A transition occurs at about 1 mbar: the high-voltage ring is covered instead of the grounded rings, accompanied by a very diffuse discharge in the full chamber volume. At 10^{-2} mbar, vacuum arcs between the rings begin and below 10^{-3} mbar gas discharge is absent.

2.2.2. Optical emission spectrocscopy

The emission spectra obtained at different gas pressures again show a transition between vacuum and gas discharges. Typical spectra are shown in Figure 5 for argon gas.

The breakdown voltage *vs* pressure curves in argon and air show a similar shape. Argon gas was used here instead of air because a monatomic spectrum is easier to interpret. In a vacuum discharge, metal vapour from the electrodes provides the medium for the discharge development. Only metal lines (mostly copper lines) are present at low pressure in the vacuum discharge zone spectrum ($p < 10^{-3}$ mbar in Figure 5). In the transition region, both metal and gas lines (argon lines) can be observed. For pressures above 10^{-2} mbar the presence of only gas lines confirms the gas discharge domination. These results confirm the distinction between gas and vacuum discharges.

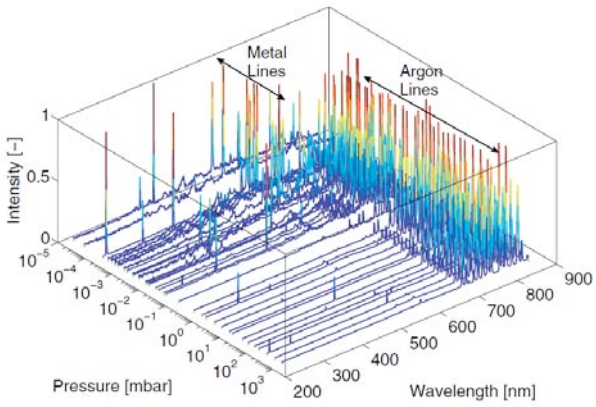

Figure 5. Optical emission spectroscopy using argon gas. Metal (mostly copper) lines are observed for pressures below 10^{-2} mbar (vacuum discharge) whereas argon lines occur for pressures above 10^{-3} mbar (gas discharge). For clarity, each spectrum is normalized to its dominant line.

2.2.3. Parameters influencing the breakdown voltage

A test campaign was conducted on representative SRA geometry, see Figure 6, in the course of which the impact of several parameters were studied in regard of arc ignition risks. The sub-assemblies basically consist of several conductors separated by typical dielectrics using a design similar to the one applied in typical SRA at RUAG Space. Different conductor materials and insulation materials were used. The parameters are the:

- Gas type (Ar, N_2, Air)
- Insulating materials (Ultem®, Macor®, vetronite)
- Insulating barriers height (0 and 2 mm)
- Conductive ring thickness (1, 2 and 4 mm)
- Housing diameter
- Voltage polarity
- Voltage pulse duration

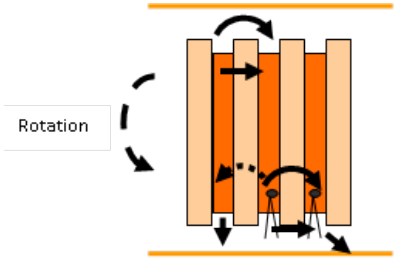

Figure 6. Possible breakdown paths in a SRA

The breakdown curve shape is observed to be almost invariant. Many different experimental parameters had no significant influence on the vacuum discharge breakdown voltage, the critical pressure, nor the gas discharge curve. An example is given in the Figure 7. The only significant impact of insulating barriers is observed for vacuum breakdown zone.

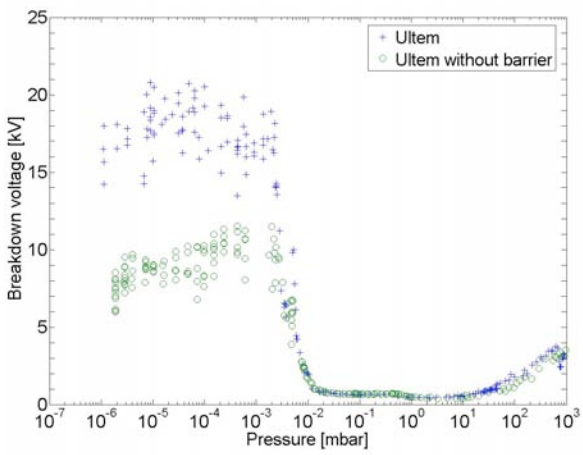

Figure 7. Measured breakdown voltage with and without Ultem® insulating barriers

2.3. NUMERICAL SIMULATION OF GAS BREAKDOWN

The experimental breakdown voltage versus pressure plot for the ring assembly geometry has the same general shape shown in Figure 3 independent of gas type. In order to explain this shape a numerical simulation model of dc breakdown in air was developed.
The simulations are calculated with the finite element software COMSOL on parallel plate, double gap, multi-gap and finally the ring assembly geometry.

2.3.1. Parallel plates extended to two gap geometry and multi-gap

As a first step to understand breakdown in complex geometry, it is helpful to consider a double gap geometry as shown in Figure 8 which is an axisymmetric geometry with a 1mm central gap (d_1) surrounded by a 100mm gap (d_2). These dimensions were chosen in accordance with the shortest and longest electric field line lengths in the ring assembly geometry. The 100mm gap corresponds approximately to the distance from the anode ring to the farthest cathode, whereas the 1mm gap represents the smallest distance between two conductor rings. In Figure 8 (*a*), the electrodes are separated by an insulating wall and therefore electric field lines are vertical, so there are only two distinct path lengths for breakdown. If the insulating wall is replaced by a conductor as in Figure 8 (*b*), the geometry can be considered to be multi-gap because all path lengths between 1 and 100mm are available for breakdown as shown by the curved electric field lines.

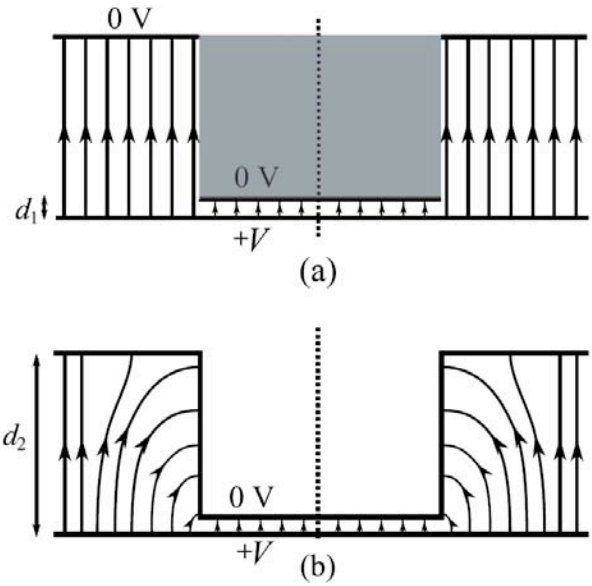

Figure 8. Schematic of cylindrically-symmetric double gap (d1 and d2) geometry showing schematic electric field lines between the electrodes drawn from COMSOL calculations. The base electrode is at positive potential V and the other electrodes are grounded.
(a) Double gap geometry: insulator separation (grey region)between the two gaps leading to only two electric field path lengths.
(b) Multi-gap geometry: all surfaces are conductors and therefore many electric field path lengths are available for breakdown.

Figure 9 shows the calculated breakdown voltages versus pressure for single gap parallel plates geometries (1 and 100 mm) compared to the double and multi-gap geometries in Figure 8 (*a*) and (*b*).
Breakdown voltages are shown as a function of pressure, not pressure times distance as in Paschen curves, because these geometries present more than a single breakdown path. Expressed as a function of pressure times gap width, breakdown voltage curves for parallel plate geometries with single gap widths of 1 and 100mm are superposed (Paschen curves). In Figure 9 these curves are shifted by a factor corresponding to their gap width. For gas pressures above 1 mbar, double gap geometry breakdown voltages correspond to 1 mm single gap ones. In fact, breakdown occurs in the smallest gap of the double gap at these high gas pressures because breakdown in the 100 mm gap needs a much higher voltage than in the 1 mm gap as shown in Figure 9. For gas pressures below 1 mbar, breakdown is located in the 100mm gap because lower voltage is needed for breakdown in bigger gaps than for smaller gaps for such low gas pressures. For the double gap geometry in Figure 8 (*a*), the locus of the breakdown curve therefore follows the lowest values of the 1 and 100 mm Paschen curves. The breakdown switches from one gap to the other as the pressure changes across the curve intersection near 1 mbar.

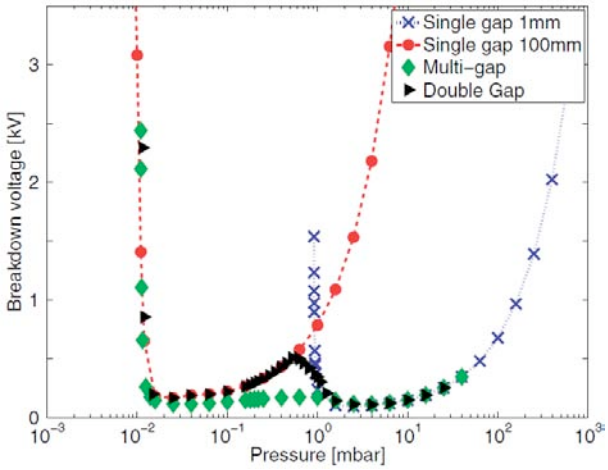

Figure 9. Calculated breakdown voltage versus pressure curve for1mm single gap, 100mm single gap, double gap and multi-gap geometry.

The same explanations can be used to describe the breakdown voltages for the multi-gap geometry in Figure 8(*b*). Breakdown occurs in the gap which needs the least voltage for breakdown compared to the other gaps. Contrary to double gap geometry, the multi-gap offers not only 1mm and 100 mm breakdown paths but also every distance in between. This explains the constant minimum breakdown voltage from 0.02 to 1 mbar in Figure 9. At higher and lower gas pressures, the breakdown is located, respectively, in the smallest and biggest gap of the double gap geometry.

2.3.2. Complex geometry: ring assembly

Figure 10 shows the experimental and the simulated breakdown voltages versus pressure for the ring assembly.

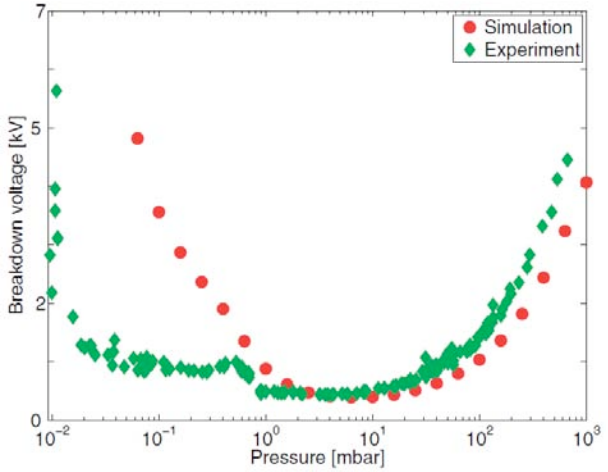

Figure 10.
Experimental and simulation breakdown voltage versus pressure for the ring assembly geometry. The experimental values are the same as in Figure 3 in air for the gas discharge region.

As in the multi-gap geometry, the breakdown voltage remains relatively constant over a wide range of

intermediate pressures due to many possible breakdown path lengths. Nevertheless, for high and low pressures, the simulation results give lower and higher breakdown voltages than the experimental ones. The parameters chosen in the simulation are probably the reason for the difference in breakdown voltage between simulation and experiment.
The uncertainty in the values for parameters means that the numerical simulation cannot give precise predictive results for the experimental breakdown voltage, but it is still useful to understand the general shape of the breakdown curve.

2.4. EXPERIMENTAL STUDY CONCLUSIONS

Breakdown voltage investigations for a complex geometry showed not only gas discharges above 10^{-2} mbar but also discharges governed by vacuum discharge mechanisms below 10^{-3} mbar. Between 10^{-3} and 10^{-2} mbar both mechanisms act together. A numerical simulation based on a fluid model was developed for breakdown simulation in air. Starting from the understanding of breakdown in simple geometries like single gaps, the overall shape of breakdown voltage versus pressure has been clarified for more complex geometries such as double and multi-gap geometries. The constant voltage zone near the minimum breakdown voltage finds its origin in the multiple discharge path availability in complex geometries. The low (high) pressure thresholds are determined by the longest (shortest) electric field path length where breakdown occurs.

2.4.1. Arc ignition lessons learnt

- The slipring is robust except from ~0.02 to ~50 mbar where the breakdown voltage is lower than 1000 V_{DC} with a minima below 500 V_{DC}.
- Surface conditioning increases the breakdown voltage at low pressure.
- A close-fitting housing increases the critical low pressure.
- A modulated voltage (up to 10 kHz) gives the same breakdown voltage as for DC over the full pressure range. Above 10 kHz breakdown voltages are higher.
- Slip ring rotation has no influence on breakdown.
- No influence of the conducting ring thickness.
- In the gas discharge region, the insulating barriers do not impact the breakdown voltage.
- In the vacuum region, the voltage breakdown is always higher than 5 kV independently of the parameters listed in §2.2.3.
- The breakdown voltage is higher for voltage pulses less than 50 μs giving possible enhanced protection against very short pulses such as ESD (Electro-Static Discharge) events.

3. ELECTRICAL MODELLING, SIMULATION AND TESTING

The SRA is a component placed inside the PSS that could be compared to a switching power supply. The PSS bloc diagram is constituted by the following elements as shown in Figure 20 and listed below:

- Solar Array Simulator
- Electrical RLC equivalent line
- Slipring assembly
- Sequential Shunt/Serial Switching Regulator
- The load representing the spacecraft consumption

The serial and the parallel (shunt) structures of S3R are modelled and simulated. Their typical structure are presented below in the Figure 11 and Figure 12.

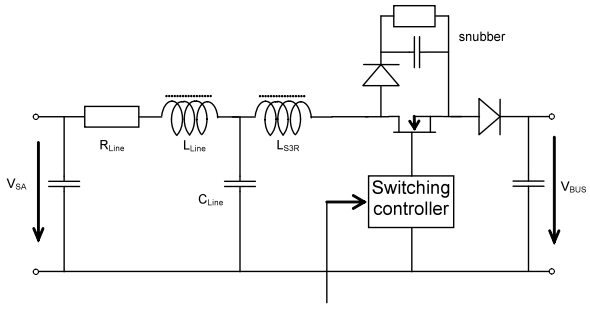

Figure 11. Sequential Serial Switching Regulator

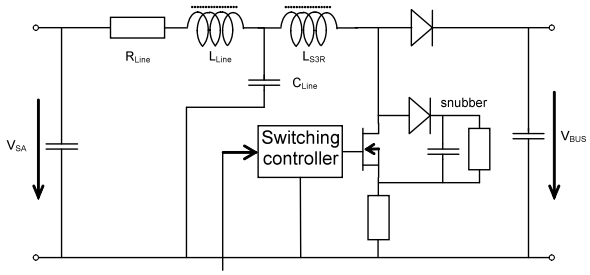

Figure 12. Sequential Shunt Switching Regulator

3.1. RESULTS and DISCUSSION

The simulations and the measurements are performed for the both serial and shunt S3R structures by varying the electrical parameters. The adequacy of the measured and the simulated results is verified.

3.1.1. Serial S3R simulation and test results

Two situations are simulated and measured, one without snubber and one with a matched snubber, see Figure 13. The obtained curves are presented in the Figure 14 and Figure 15. It was observed the importance of the adequate design of the snubber circuit in the serial structure unless an important overvoltage can be present at SRA level , see Figure 14. In the Figure 15 the positive effect of the snubber is demonstrated.
The overvoltage is according to:

$$u(t) = L \cdot \frac{di}{dt} \qquad (1)$$

The equation (1) shows the importance to minimize

the value of the line inductance. Nevertheless by adding an appropriate snubber, the overvoltage will be cancelled. The power loss in the snubber, equation (2) is directly link to the value of the inductance, that is an additional reason to minimize its value by an appropriate cabling.

$$P_{LOSS} = \frac{1}{2} \cdot L \cdot I^2 \cdot f_{Switching} \qquad (2)$$

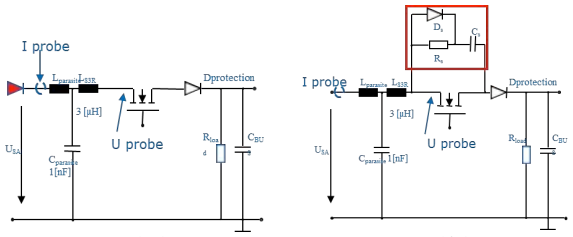

(a) *(b)*

Figure 13. Serial Switching regulator; without (a) and with (b) snubber circuit

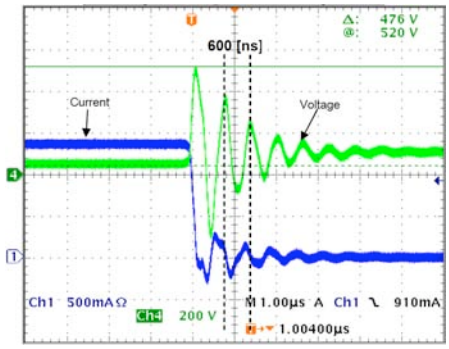

Figure 14. Serial Switching current and voltage curves without snubber

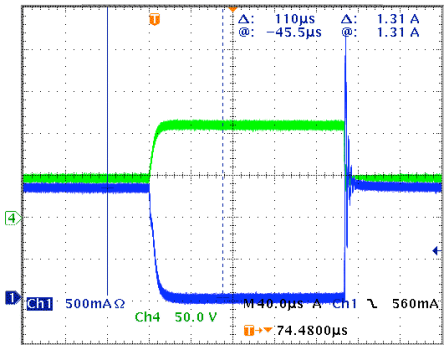

Figure 15. Serial Switching current and voltage curves with well-matched snubber

3.1.2. Parallel S3R simulation and test results

A shunt regulator model is presented in Figure 16. The results of the simulation and the measurements are perfectly matching. In this situation, we don't observe any overvoltage who can lead to a voltage breakdown in the SRA. An inrush current is due to the source output capacitor. A snubber is then not needed.

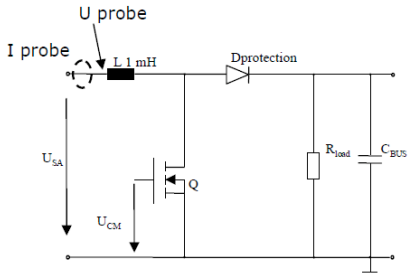

Figure 16. Shunt Switching regulator

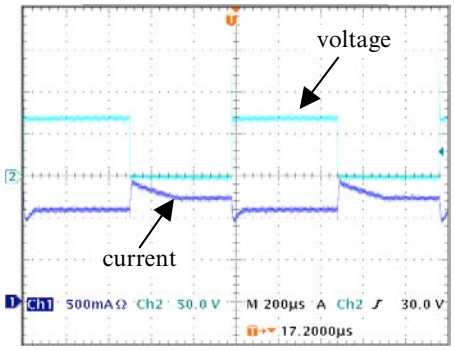

Figure 17. Shunt Switching current and voltage measured curves

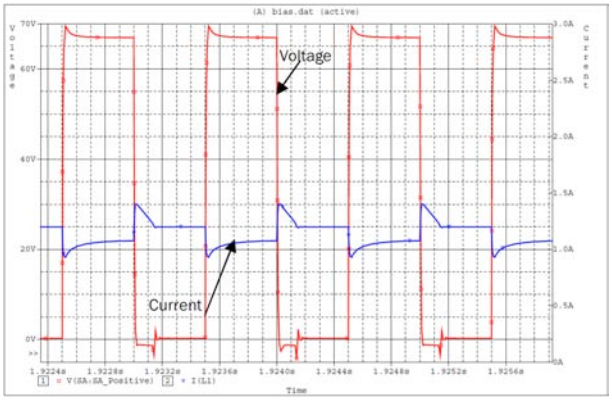

Figure 18. Shunt Switching current and voltage simulated curve

3.1.3. Lessons learnt

- The tests and simulations have shown that the line inductance and capacitance (line impedance) represent an important parameter in the evaluation of the voltage spikes appearing on the serial S3R bus regulator.
- The tests and layout experimented on the pulse generators have shown that ringing effects, resulting in over-voltage and current spikes after each switching of the S3R, are significantly reduced, when using low speed switching devices, according to the equation (1).
- The simulations and measurements have confirmed that using a serial S3R presents much higher voltage spike amplitudes than using the

parallel S3R.

- The design of a snubber circuit lowers or even suppresses the over-voltage spikes generated by the switching of the serial S3R.
- S3R configurations having a large input inductance (significantly larger than the equivalent line inductance) will present a more robust behaviour versus line parameters and SA-impedance.
- Serial S3R configurations may present over-voltage spikes on the SRA, whereas shunt S3R configurations do present over-current spikes through the SRA (without over-voltage spikes phenomena).
- The static and dynamic characteristics of the SA (Solar array) have a minor influence on the current and voltage shape appearing on the SRA, thus compared to the line parameters and the switching parameters

4. TEST BENCH DEVELOPMENT

A complete test bench has been developed in collaboration with swiss academic partners and main European SADM manufacturers. It permits to perform functional tests and voltage breakdown test.

Figure 19. Functional and voltage breakdown test bench (TVAC and interfaces)

4.1. FUNCTIONAL TEST BENCH DESCRIPTION

The SRA is part of the PSS of the spacecraft and it is of prime importance to test the entire electrical system as presented in Figure 20.

The objective of the test bench development is to have the possibility to place a slipring in an electrical situation as close as possible as the flight configuration. It means that it will be connected at its both end with representative electrical interfaces and components. In summary one side will be connected to a SAS through electrical line and the other side will be connected to the S3R and a load.

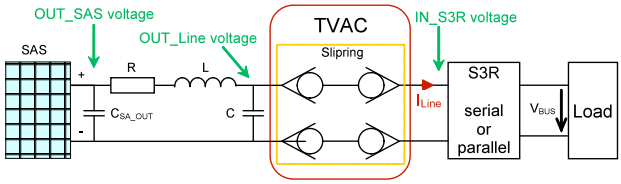

Figure 20. Functional SRA test configuration

The parameters are:

- Gas type (N_2, Air)
- Pressure
- Temperature
- DC bus voltage
- Line current
- RLC values (line characteristics)
- S3R switching type (serial or parallel)
- S3R switching frequency
- Power MosFet snubber circuit (active or not)
- Measurement time

The number of possible measurements is quite infinite. Nevertheless a selection of relevant combinations have been tested. Two examples of serial S3R are given in the
Figure *21* and
Figure *23* where we can see the voltages and current as follows:

Channel 1	Output_SAS voltage
Channel 2	Output_Line voltage
Channel 3	Input_S3R voltage
Channel 4	Line current

The over-voltages when the snubber is active are very limited even with a big value of inductance.

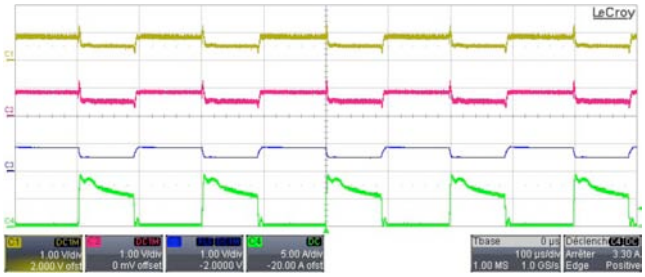

Figure 21. Curves for serial S3R with:
Type of gas : Air
Pressure: 10E-6 [mbar]
Temperature: 40 [°C]
Ubus voltage: 50 [VDC]

Ibus: 3 [A_{dc}]
Switching frequency: 5 [kHz]
Line values: R=0.1 Ω; L=6 µH; C=400 pF
Serial snubber circuit : active

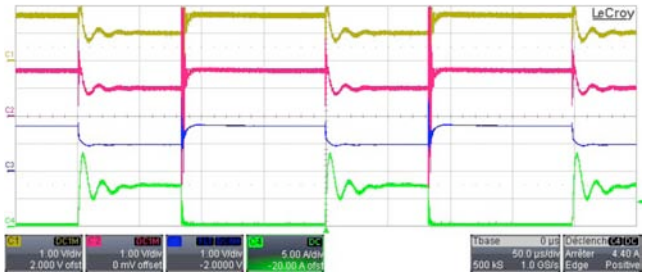

Figure 23. Curves for serial S3R with:
Type of gas : Air
Pressure: 10E-6 [mbar]
Temperature: 40 [°C]
Ubus voltage: 100 [VDC]
Ibus: 3 [A_{dc}]
Switching frequency: 5 [kHz]
Line values: R=0.25 Ω; L=10 µH; C=250 pF
Serial snubber circuit : not active

An example with a shunt S3R is given in the Figure 25, we observe an absence of over-voltages. The inrush currents at the switching points is due to the line capacitance.

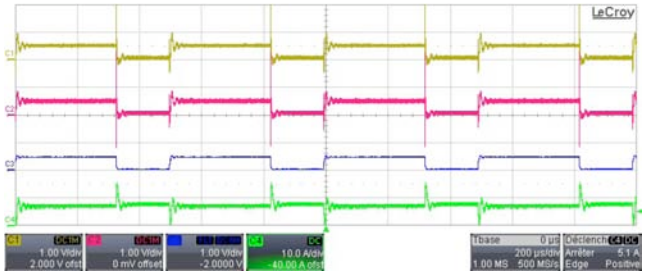

Figure 25. Curves for parallel S3R with:
Type of gas : Air
Pressure: 10E-6 [mbar]
Temperature: 40 [°C]
Ubus voltage: 50 [VDC]
Ibus: 4.6 [A_{dc}]
Switching frequency: 2 [kHz]
Line values: R=0.25 Ω; L=10 µH; C=250 pF

4.2. BREAKDOWN VOLTAGE TEST BENCH DESCRIPTION

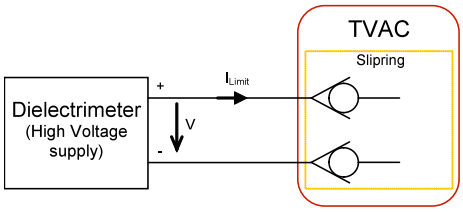

Figure 26. Breakdown SRA voltage test configuration

5. This test bench configuration permits to obtain the Paschen curve of a SRA. An example is given in the

Figure ***27***. The Dielectrimeter is a Sefelec DMG50 serie. This curve is a typical Paschen curve of two rings of a SRA. We observe a minima below 400 Vdc over one pressure decade that represents the critical gas effect zone described above in the document.

The voltage breakdown test bench is fully automatic (including a report generation) and need only to enter the following parameters before to start the measurements:

- Operator identification
- Device identification
- Type of gas
- Pressure min [mbar]
- Pressure max [mbar]
- Tolerance pressure [+- %]
- Pressure number of points/decade
- Test temperature [°C]
- Voltage [Vdc]
- I Limit [A]

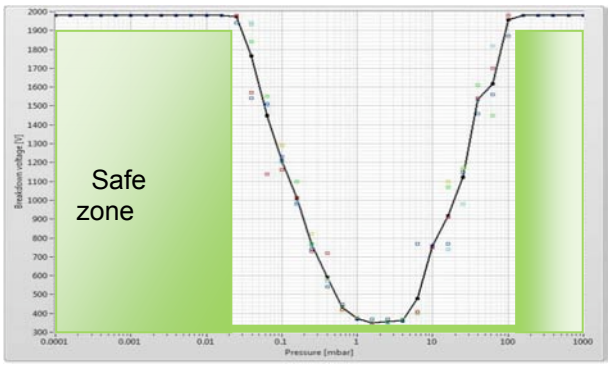

Figure 27. Breakdown voltage measurement with:
Type of gas : Air
Pressure: 100E-6 .. 1000 [mbar]
Temperature: 40 [°C]
Voltage max: 2000 [VDC]
I_{limit}: 100 [µA_{dc}]

The typical safe zone for this curve is represented in green.

6. SRA QUALIFICATION

In the frame of the RETS project a full SRA qualification is performed with the developed test bench in association with existing RUAG Space test benches. The test sequence is given in the Figure 29. The tests that are performed with the help of the test bench developed in the frame of the RETS project are highlighted in red. The so called switching tests are in the fact the functional tests as described in §4.1.

The SRA used for the qualification has numerous configurations with:

- various insulating barriers materials and dimensions
- two types of cables.
- two types of tracks materials.
- insulating tubes on the brushes for half of the tracks.

The obtained results in regard of arcing ignition risks are homogeneous. Then it is not observed significant improvements to high voltage robustness depending to these different configurations.

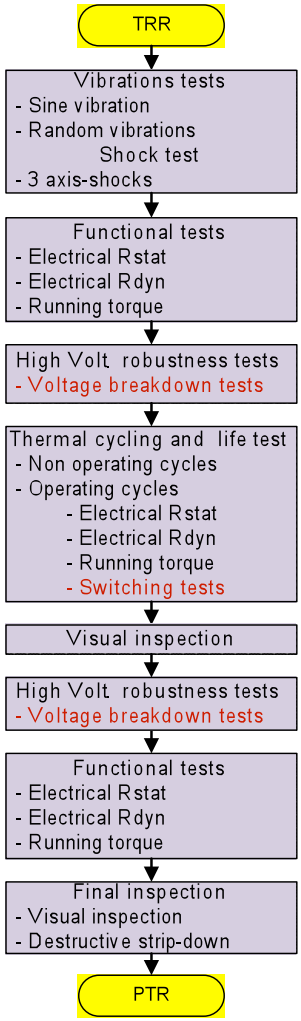

Figure 29. SRA qualification test sequence.

7. CONCLUSIONS AND GUIDELINES

The RETS project was split in three phases. An experimental phase where the physics of the voltage breakdown was studied and experimented. The parameters influencing the arcing ignition were identified and validated through scientific experiments and simulations.

A second phase while electrical interfaces simulations and measurements was performed on a complete spacecraft PSS model. Simulations and experimental measurements have permit to understand the role of the components and the parameters linked to the arcing risk occurrence in a SRA.

A third phase was dedicated to the test bench development and its validation on elementary models and a complete SRA qualification.

6.1. GUIDELINES FOR THE PSS DESIGN INCLUDING A SRA

The lessons learnt from the entire RETS project

permit to propose guidelines for the SRA and for the system designs.

At the SRA level design, the main points are:
- To have a close confinement of the slipring. It is advised to close the windows, if any, with conductive covers or to have a fully closed housing.
- To consider additional insulators, like brush insulation tubes or adhesive sheets on the housing as not necessary to prevent voltage breakdown in operational conditions.

At the PSS level, it is advised for the electrical designers to consider the following points :
- To minimize the line inductance by an appropriate cabling implementation.
- To adapt the snubber circuits of the serial S3R to their respective solar array sections.
- To avoid as far as possible to have voltage above 300Vdc on SRA level over the entire pressure range.
- To test the complete PSS in representative conditions as presented in 4.1.
- To test and characterize the SRA arcing robustness as presented in 4.2.

8. REFERENCES

1. R. Schnyder, A. Howling, D. Bommottet, Ch. Hollenstein. Direct current breakdown in gases for complex geometries from high vacuum to atmospheric pressure. *JOURNAL OF PHYSICS D: APPLIED PHYSICS 46 (2013) 285205 (9pp)*